

Deformable image registration of CT images for automatic contour propagation in radiation therapy

Qian Wu^{a,b,c,d,e}, Ruifen Cao^{b,c,e}, Xi Pei^{b,c,e}, Jing Jia^{b,c,e} and Liqin Hu^{a,b,c,e,*}

^a*University of Science and Technology of China, Hefei, Anhui 230027, China*

^b*Key Laboratory of Neutronics and Radiation Safety, Institute of Nuclear Energy Safety Technology, Chinese Academy of Sciences, Hefei 230031, China*

^c*Engineering Technology Research Center of Accurate Radiotherapy of Anhui Province, Hefei 230031, China*

^d*School of General Education, Anhui Medical University, Hefei, Anhui 230032, China*

^e*Collaborative Innovation Center of Radiation Medicine of Jiangsu Higher Education Institutions, Suzhou 215006, China*

Abstract. Radiotherapy treatment plan may be replanned due the changes of tumors and organs at risk (OARs) during the treatment. Deformable image registration (DIR) based Computed Tomography (CT) contour propagation in the routine clinical setting is expected to reduce time needed for necessary manual tumors and OARs delineations and increase the efficiency of replanning. In this study, a DIR method was developed for CT contour propagation. Prior structure delineations were incorporated into Demons DIR, which was represented by adding an intensity matching term of the delineated tissues pairs to the energy function of Demons. The performance of our DIR was evaluated with five clinical head-and-neck and five lung cancer cases. The experimental results verified the improved accuracy of the proposed registration method compared with conventional registration and Demons DIR.

Keywords: Computed tomography, deformable image registration, structure delineation, contour propagation

1. Introduction

Radiation Therapy (RT) is one of the main cancer treatment modality, and is applied in more than 50% of all cancer cases. It aims to more precisely target tumors while protecting the surrounding critical normal tissue. Imaging has become the primary source of information in the treatment processing of RT. For example, the use of imaging to accurately delineate tumors and OARs, particularly the use of CT has led to improved precision in target localization. However, the precision of targeting is affected by great changes in the location, shape and size of tumors and OARs during RT treatment due to respiratory movement, weight loss, and tumor shrinkage. It is then necessary to re-

* Address for correspondence: Liqin Hu, Institute of Nuclear Energy Safety Technology, Chinese Academy of Sciences, Hefei 230031, China. Tel.: +1 160 65593590; Fax: +1 610 6559 3681; E-mail: liqin.hu@fds.org.cn.

contour tumors and OARs, which requires a significant amount of time for radiation oncologists to manually delineate tumors and OARs for each CT image. Deformable image registration (DIR) is a process to precisely map the data collected at different times or with different image modalities into a single coordinate system, typically that of planning CT. Moreover, deformation vector field (DVF), which is the result of registration, can be utilized to automatically delineate tumors and OARs with CT-to-CT images contour propagation.

Many DIR methods have been proposed, such as the optical flow method, Finite Elements Methods (FEM), B-spline method and the Demons method. Among these, Demons has been proved to be an efficient and robust DIR method. For example, SmartAdapt (v11, Varian Medical System) utilizes an accelerated Demons-based DIR method, and Pinnacle Syntegra (v9.710, Philips Healthcare) uses a B-spline-and Demons-based DIR method. However, Demons is not suitable for images with large deformations and multi-modality images. Demons invariants have been proposed; for example, M. Modat, et al. [1] proposed a diffeomorphic Demons method using normalized mutual information. An intensity-based Demons image registration method is suitable for CT images in radiotherapy applications due to the image intensity consistency of CT. Furthermore, prior structure delineations are incorporated into Demons DIR, which is a variant of the Demons method with a similar objective function modified by an additional regularization term of the contours of tumors and OARs. The clinical workflow chart for contour propagation from delineated contours on planning CT (pCT) to treatment CT (tCT) using DIR method is displayed in Figure 1.

2. Methods

2.1. The basis of Demons

The Demons algorithm regards registration as a diffusion process from the floating image to the reference image. First, a displacement vector d is calculated at all voxel points. The result is then convolved by 3D Gaussian Kernel function to smooth the deformation field. Next, the incremental vector Δd is added to the existing deformation field $d(x)$ and the floating image is updated. Many types of Demons variants were developed with the calculation of DVF as the primary improvement. We

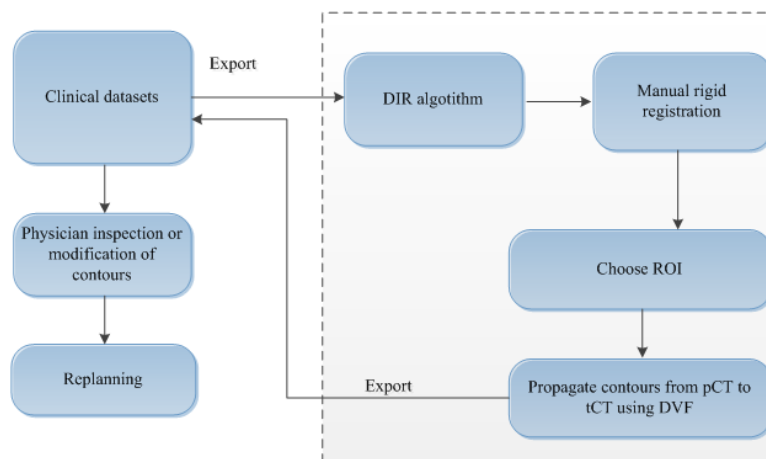


Fig. 1. Workflow diagram for CT-to-CT contour propagation.

investigated four ITK based Demons variant algorithms and found that the performance of the symmetric Demons implemented by Vercautern [2] was advantageous over the original Demons and the other two Demons variants. The symmetric Demons defines the displacement field as follows:

$$\Delta d_r^{i+1}(x) = \frac{2(m^i(x)-f(x))(\nabla m^i(x)+\nabla f(x))}{\|\nabla m^i(x)+\nabla f(x)\|^2+(m^i(x)-f(x))^2/K^2} \quad (1)$$

where $m^i(x)$ and $f(x)$ respectively represent the moving image after the i th iteration and the fixed image; $\nabla m^i(x)$ and $\nabla f(x)$ denote the gradient image; and K^2 is the mean-squared value of the image voxel size.

2.2. Prior delineation of CT based DIR method

Demons is a process of optimizing the displacement of every pixel in the floating image to accurately construct point-to-point correspondence of the registered images, which can be mathematically represented by two terms of a similarity measurement and regularization of DVF:

$$\begin{aligned} E(u) &= \frac{1}{\sigma_i^2} S(F, M \circ u) + \frac{1}{\sigma_T^2} Reg(u) \\ &= \frac{1}{\sigma_i^2} \|F - M \circ u\|^2 + \frac{1}{\sigma_T^2} \|\nabla u\|^2 \\ u &= \arg \min(E(u)) \end{aligned} \quad (2)$$

where $M \circ u$ transforms the points of the moving image into the coordinate of the fixed image by the spatial transformation u ; σ_i^2 accounts for the noise on the image intensity; and σ_T^2 controls the amount of necessary regularization. An image similarity term measures the similarity of the two registered images. The mean square error (MSE) metric, which is suitable for mono-modality image registration, was utilized in our work; the deformation field was regularized to obtain the only DVF.

In RT processing, temporal variations are the predominant source of treatment uncertainty, because shape and position of the patient or organs could vary during the fraction treatment. In the DIR for RT, pCT was used as the fixed image acquired before the treatment, and tCT was the moving image collected after 3-4 weeks of treatment. The geometrical information provided by the delineated contours of pCT images and the edited contour of tCT images were integrated into Demons. Given a collection of N pairs of pCT-tCT contours of tumors and OARs, a deformation field could be computed that maps the pCT contours to the tCT contours by optimizing the energy function:

$$\begin{aligned} E(u) &= E_{struc}(u) = \frac{1}{\sigma_i^2} \cdot \frac{1}{N} \sum_{i=1}^N S(R_i, F_i \circ u) + \frac{1}{\sigma_T^2} Reg(u) \\ FR_i &= \left(1 + \frac{K_i(x)}{2}\right) \cdot R, \quad K_i(x) = \begin{cases} 0 & x \notin \Omega_i^{pCT} \\ \pm 1 & x \in \Omega_i^{pCT} \end{cases} \\ MF_i &= \left(1 + \frac{L_i(x)}{2}\right) \cdot F, \quad L_i(x) = \begin{cases} 0 & x \notin \Omega_i^{tCT} \\ \pm 1 & x \in \Omega_i^{tCT} \end{cases} \end{aligned} \quad (3)$$

where R_i and F_i individually represent contoured images with the i th delineation pair set on pCT and

tCT based on R and F ; and Ω_i^{pCT} and Ω_i^{tCT} denote a closed region enclosed by the i th contour pair on pCT and tCT. $K_i(x)$ and $L_i(x)$ are equal to zero if the pixel is not in the ROI; the values are positive if the intensity inside the closed region is higher than its surrounding, and negative when lower.

A middle variable was introduced in the registration process to translate the Demons algorithm into a minimization of a well-posed criterion [3], which deemed the regularization term as prior knowledge to smooth the transformations. Some errors were allowed in the non-parametric spatial transformation c . The global energy function can be represented as follows:

$$\begin{aligned} E(c, u) &= \frac{1}{\sigma_i^2} \cdot \frac{1}{N} \sum_{i=1}^N S(F_i, M_i \circ c) + \frac{1}{\sigma_x^2} dist(u, c)^2 + \frac{1}{\sigma_T^2} Reg(u) \\ &= \frac{1}{\sigma_i^2} \cdot \frac{1}{N} \cdot \|F_i - M_i \circ c\|^2 + \frac{1}{\sigma_x^2} \cdot \|u - c\|^2 + \frac{1}{\sigma_T^2} \cdot \|\nabla u\|^2 \\ (c, u) &= arg \min(E(c, u)) \end{aligned} \quad (4)$$

where σ_x^2 specifies a spatial uncertainty on the correspondence of the spatial transformation c and u . The optimization process consists of two steps. First, with a given u , $E_1(c) = \frac{1}{\sigma_i^2} \cdot \frac{1}{N} \cdot \sum_{i=1}^N \|F_i - M_i \circ c\|^2 + \frac{1}{\sigma_x^2} \cdot \|u - c\|^2$ was optimized from $c=u$, then the incremental vector du was calculated by minimizing $E_1(du)$.

$$E_1(du) = \frac{1}{\sigma_i^2} \cdot \frac{1}{N} \cdot \sum_{i=1}^N \|F_i - M_i \circ (u + du)\|^2 + \frac{1}{\sigma_x^2} \cdot \|du\|^2 \quad (5)$$

Second, c was deemed to be a given parameter, minimizing the energy function E which is equal to optimized $E_2(u) = \frac{1}{\sigma_x^2} \cdot \|u - c\|^2 + \frac{1}{\sigma_T^2} \cdot \|\nabla u\|^2$. The Gaussian smoothing kernel was adopted to convolve the deformation field u to optimize the regularization term. The moving image term was approximately expressed by Taylor expansion with a small deformation du , $M_i \circ (u + du) \approx \widetilde{M}_i + \nabla \widetilde{M}_i \cdot du$, where, $\widetilde{M}_i = M_i \circ u$ are deformed floating images with given deformation u . Then,

$$arg \min(E_1(du)) \approx \frac{1}{\sigma_i^2} \cdot \frac{1}{N} \cdot \sum_{i=1}^N \|\widetilde{M}_i + \nabla \widetilde{M}_i \cdot du - F_i\|^2 + \frac{1}{\sigma_x^2} \cdot \|du\|^2 \quad (6)$$

In Eq. (6), the incremental vector can be rewritten as $du = v \cdot n$, where v is the amplitude of the incremental vector and n is the moving direction of du . Assuming that the displacement du was projected onto $n = \frac{\nabla \widetilde{M}}{|\nabla \widetilde{M}|}$, Eq. (6) can be simplified from $du = arg \min(E_1(du))$ to $v = arg \min(E_1(v))$.

$$arg \min(E_1(du)) = arg \min(E_1(v)) \approx \frac{1}{\sigma_i^2} \cdot \frac{1}{N} \cdot \sum_{i=1}^N \|(\nabla \widetilde{M}_i \cdot n)v + \widetilde{M}_i - F_i\|^2 + \frac{1}{\sigma_x^2} \cdot v^2 \quad (7)$$

The first-order optimality condition was applied to obtain the optimal solution of Eq. (7).

$$\begin{aligned}
 \frac{\partial E_1(v)}{\partial v} &= \frac{2}{\sigma_i^2} \cdot \frac{1}{N} \cdot \sum_{i=1}^N ((\nabla \widetilde{M}_i \cdot n)v + \widetilde{M}_i - F_i) \cdot \nabla \widetilde{M}_i \cdot n + \frac{2}{\sigma_x^2} \cdot v \\
 &= \frac{2}{\sigma_i^2} \cdot \frac{1}{N} \cdot \sum_{i=1}^N (\nabla \widetilde{M}_i \cdot n)^2 \cdot v + \frac{2}{\sigma_x^2} \cdot v + \frac{2}{\sigma_i^2} \cdot \frac{1}{N} \cdot \sum_{i=1}^N (\nabla \widetilde{M}_i \cdot n) \cdot (\widetilde{M}_i - F_i) \\
 v &= \frac{\frac{1}{N} \sum_{i=1}^N (\nabla \widetilde{M}_i \cdot n) \cdot (F_i - \widetilde{M}_i)}{\frac{1}{N} \sum_{i=1}^N (\nabla \widetilde{M}_i \cdot n)^2 + \frac{\sigma_i^2}{\sigma_x^2}} \tag{8}
 \end{aligned}$$

If the local estimation of the image noise was set as $\sigma_i^2 = |F - M \circ u|^2$, the expression would be identical to the Demons forces proposed by Thirion [4]. Note that the maximum step length is relative to the choice of image noise σ_x^2 , $\sigma_x^2 = \frac{d^2}{2} \cdot (r_x^2 + r_y^2)$; d is the step length; and r_x and r_y are the resolution of the x and y axial directions, respectively.

3. Experiments and results

Ten clinical cases were evaluated to test the effect of DIR, including five head-and-neck cancer cases and five lung cancer cases. The pCT and tCT images were acquired before and during treatment with dimensions of $512 \times 512 \times 160$ and a resolution of $1.97 \times 1.97 \times 2.5 \text{ mm}^3$. There were generally great differences in the anatomy of the images after 3-4 weeks of treatment. The couch and masks had been removed from pCT and tCT images, and images had been down-sampled to $256 \times 256 \times 80$ to balance the computational time and memory capability. Figure 2 shows segmented brain and lung images.

It is difficult to evaluate the accuracy of DVF for the clinical image registration due to a lack of ground-truth. Fortunately, some information such as contour and structure could be obtained by image processing methods. For example, the computed DVF according to DIR was applied to transform the floating images including ROIs, or to propagate the contours of the reference images to the floating images. Next, the DVF accuracy was quantitatively analyzed by calculating the overlap rate of the transformed and target ROIs.

In this study, the Dice Similarity Coefficient quantitative criterion was used to validate the performance of the DIR methods, defined as $\text{Dice} = \frac{2 \times (V_1 \cap V_2)}{V_1 + V_2}$; where V_1 is a deformed ROI and V_2 is the corresponding target ROI. In our work, V_1 was a propagated structure region from pCT and

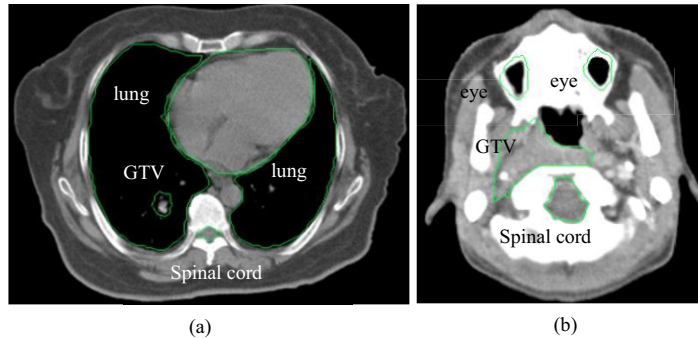


Fig. 2. Segmented images of (a) lung and (b) brain.

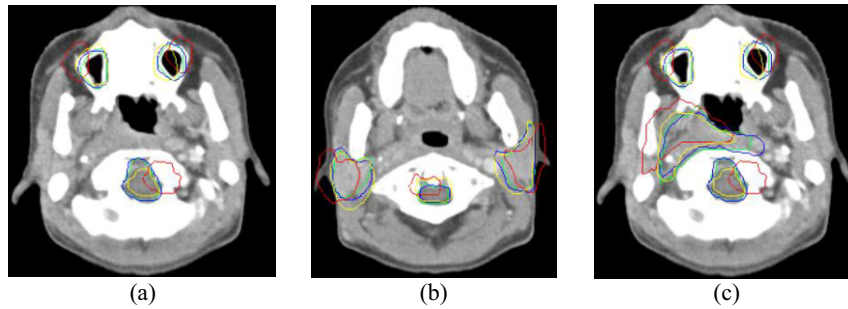


Fig. 3. Example contour propagations using different methods: (a) eyes and spinal cord (b) parotid glands and spinal cord (c) eyes, spinal cord and PTV.

V_2 represented physicians’ manually delineated regions on tCT. The more the suggested regions overlapped, the better the registration accuracy. If the ROIs were completely identical, Dice was equal to 1; if there was no overlap, Dice was equal to 0.

The second evaluation method was comparing contours of GTV and ROI, which propagated from pCT to tCT using the calculated DVF. In this paper, two example contour propagation cases were presented using the rigid registration method, manual contour method, Demons method and our DIR method, which were respectively represented with a red line, blue line, yellow line and green line. For brain cases, contours of only the spinal cord, eyes, parotid glands and GTV were shown; the spinal cord and GTV were included in lung cases for improved visibility. A head-and-neck case is shown in Figure 3. From the figures, we determined that there was great discrepancy between manual delineated contours on tCT as identified by physicians and the contour propagation to pCT by rigid registration. The differences between the contours mapped on pCT by Demons DIR and the ground-truth was obviously reduced. Further, mapping pCT contours by our method and manually drawn contours were overlaid on tCT images. The average Dice value was approximately 0.74 for parotid glands by applying rigid registration to map contours on tCT, compared to approximately 0.92 achieved by Demons deformed ROIs; the value increased to approximately 0.99 when deforming ROIs with our

Table 1

Dice coefficients for the brain case 2 with different registration methods

		Rigid registration	Symmetric Demons	Proposed method
2	Eye R	0.5372	0.9120	0.9976
3	Spinal cord	0.6478	0.9205	0.9915
4	parotid glands	0.7931	0.9210	0.9938
5	GTVs	0.8016	0.9021	0.9930

Table 2

Overall mean±standard deviation Dice coefficients for five brain cases with different registration methods

		Rigid registration	Symmetric Demons	Proposed method
1	Eye L	0.5121±0.0353	0.9004±0.0200	0.9899±0.0100
2	Eye R	0.5362±0.0160	0.9130±0.0127	0.9937±0.0053
3	Spinal cord	0.7487±0.0135	0.9205±0.0133	0.9902±0.0043
4	Parotid glands	0.7875±0.0121	0.9227±0.0084	0.9912±0.0043
5	GTVs	0.8090±0.0107	0.9018±0.0033	0.9926±0.0064

method as listed in Tables 1 and 2.

Further evaluation was conducted on five lung cases. As noted in Figure 4, contour misalignments were evident with rigid registrations. However, the differences were mitigated after Demons DIR, and CT-to-CT propagated contours based on the proposed method were most consistent with physician delineated tCT contours. Tables 3 and 4 list the Dice values, which quantitatively verified the agreement of the contours. As listed in Table 4, the mean Dice for GTV was approximately 0.36 by rigid registration to map contours. The values of Dice increased to approximately 0.70 by Demons deformed ROIs, and values of Dice further increased to approximately 0.98 when transforming ROIs with the proposed method.

4. Conclusions

A DIR method based on prior structure delineation was developed for CT-to-CT contour propagation in radiotherapy and validated by clinical cases. Contours were incorporated into Demons DIR to deform the moving images, and the propagated contours were the most consistent with physician manually delineated contours compared to other registration methods, such as rigid registration and Demons DIR. The average computational time of the proposed method was approximately 35 minutes (the size of CT was down-sampled to 128×128×40) with CPU. Next, we will attempt to speed up the proposed method and aim to apply our ARTS-IGRT system [4-13] to clinical practice. In addition to the processing time, automatic contour propagation could be applied not only to mono-modality images (such as CT-to-CT), but also to multi-modality images (such as CT-to-MR). The respiratory motion is one of the largest factors of uncertainty in RT, which should also be considered in radiotherapy treatment planning.

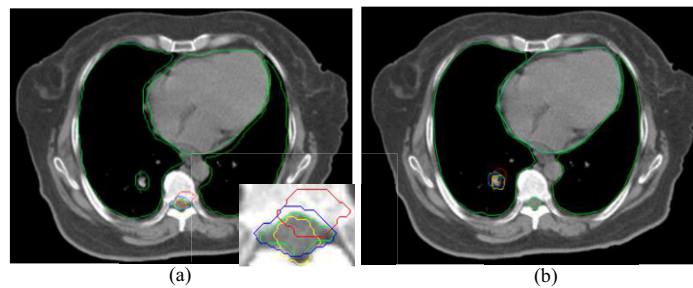


Fig. 4. Example contour propagations using different methods: (a) spinal cord (b) PTV.

Table 3

Dice coefficients between physicians' manually delineated parotids/GTV and mapped volumes for lung cases

		Rigid registration	Symmetric Demons	Proposed method
1	Spinal cord	0.3387	0.6605	0.9942
2	GTVs	0.4016	0.7251	0.9805

Table 4

Overall mean±standard deviation Dice coefficients for five lung patients using different registration methods

		Rigid registration	Symmetric Demons	Proposed method
1	Spinal cord	0.3696±0.0338	0.6805±0.0633	0.9822±0.0173
2	GTVs	0.3776±0.0349	0.7053±0.0249	0.9810±0.0152

Acknowledgments

This paper was supported by National Magnetic Confinement Fusion Science Program of China (No. 2014GB112000), National Natural Science Foundation of China (No. 11305203) and Anhui Provincial Natural Science Foundation (No. 1508085QH180). Moreover, authors would like to thank the great help from other members of FDS Team.

References

- [1] M. Modat, T. Vercauteren, G.R. Ridgway, et al., Diffeomorphic demons using normalized mutual information: Evaluation on multimodal brain MR images, *Medical Imaging* **55** (2010), N465-N471.
- [2] X. Gu, H. Pan, Y. Liang, et al., Implementation and evaluation of various Demons deformable image registration algorithms on a GPU, *Physics in Medicine and Biology* **55** (2010), 207-219.
- [3] P. Cachier and N. Ayache, Isotropic energies, filters and splines for vector field regularization, *Journal of Mathematical Imaging and Vision* **20** (2004), 51-65.
- [4] R.F. Cao, Y.C. Wu, X. Pei, et al., Multi-objective optimization of inverse planning for accurate radiotherapy, *Chinese Physics C* **35** (2011), 297-313.
- [5] Y.C. Wu, G.L. Li and S.X. Tao, The research and development of accurate/advanced radiotherapy treatment planning system (ARTS), *Chinese Journal of Medical Physics* **22** (2006), 683-690.
- [6] Y.C. Wu and FDS Team, Conceptual design activities of FDS series power plants in China, *Fusion Engineering and Design* **81** (2006), 2713-2718.
- [7] Y.C. Wu and FDS Team, Conceptual design of the China fusion power plant FDS-II, *Fusion Engineering and Design* **83** (2008), 1683-1689.
- [8] Y.C. Wu, J. Song, H.Q. Zheng, et al., CAD-based Monte Carlo program for integrated simulation of nuclear system SuperMC, *Annals of Nuclear Energy* **82** (2015), 161-168.
- [9] Y.C. Wu, G. Song, R.F. Cao, et al., Development of accurate/advanced radiotherapy treatment planning and quality assurance system (ARTS), *Chinese Physics C (HEP & NP)* **32** (2008), 177-182.
- [10] Y.C. Wu, J. Jiang, M. Wang, et al., A fusion-driven subcritical system concept based on viable technologies, *Nuclear Fusion* **51** (2011), 103-106.
- [11] Q. Huang, D. Li, M. Chen, et al., Progress in development of China low activation martensitic steel for fusion application, *Journal of Nuclear Materials* **367** (2007), 142-146.
- [12] L. Qiu, Y.C. Wu, B. Xiao, et al., A low aspect ratio Tokamak transmutation system, *Nuclear Fusion* **40** (2000), 629-633.
- [13] Y.C. Wu and FDS Team, CAD-based interface programs for fusion neutron transport simulation, *Nuclear Science and Engineering* **84** (2009), 1987-1992.